Posterior heart field and epicardium in cardiac development : PDGFRα and EMT

Bax, N.A.M.

PART 2

EPDCs in epithelial-to-mesenchymal transformation and cardiomyocyte differentiation

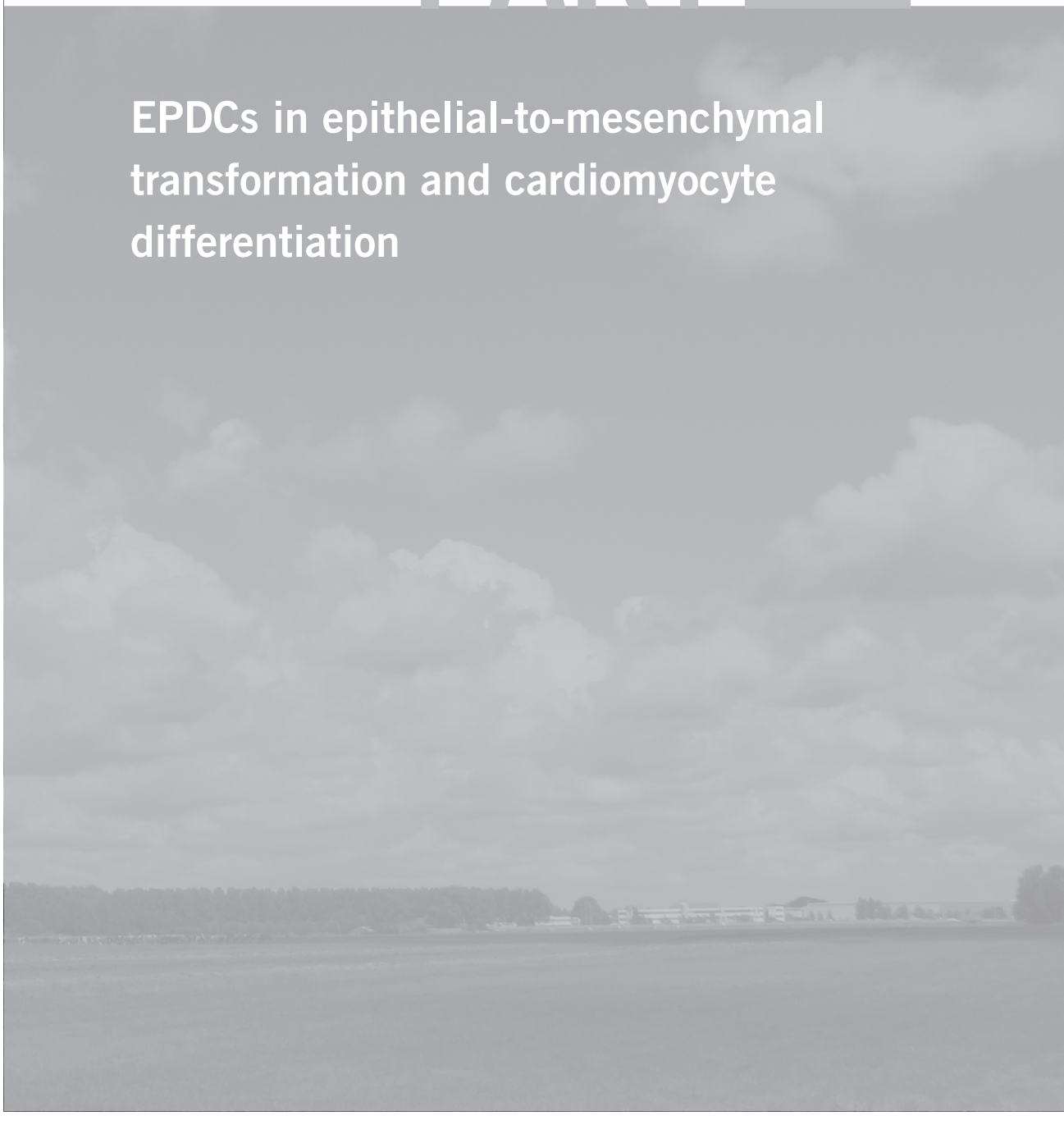

CHAPTER 5

Epicardium-derived cells enhance proliferation, cellular maturation and alignment of cardiomyocytes

Noortje A.M. Bax[1], Alida Weeke-Klimp[2]*, Anna Rita Bellu[2], Elizabeth M. Winter[1], Johannes Vrolijk[3], Josée Plantinga[2], Saskia Maas[1], Marja Brinker[2], Edris A.F. Mahtab[1], Adriana C. Gittenberger-de Groot[1], Marja J.A. van Luyn[2], Martin C. Harmsen[2], Heleen Lie-Venema[1]*

** Both authors contributed equally to this study.*

1 Department of Anatomy and Embryology, Leiden University Medical Center, The Netherlands
2 Department of Pathology and Medical Biology, Medical Biology section, Stem Cell and Tissue Engineering Group, University Medical Center Groningen, University of Groningen, The Netherlands
3 Department of Molecular Cell Biology, Leiden University Medical Center, The Netherlands.

Modified after Journal of Molecular and Cellular Cardiology 2010;49:606-616

ABSTRACT

During heart development, cells from the proepicardial organ spread over the naked heart tube to form the epicardium. From here, epicardium-derived cells (EPDCs) migrate into the myocardium. EPDCs proved to be indispensible for the formation of the ventricular compact zone and myocardial maturation, by largely unknown mechanisms.

In this study we investigated *in vitro* how EPDCs affect cardiomyocyte proliferation, cellular alignment and contraction, as well as the expression and cellular distribution of proteins involved in myocardial maturation. Embryonic quail EPDCs induced proliferation of neonatal mouse cardiomyocytes. This required cell-cell interactions, as proliferation was not observed in transwell cocultures. Western blot analysis showed elevated levels of electrical and mechanical junctions (connexin43, N-cadherin), sarcomeric proteins (Troponin-I, α-actinin), extracellular matrix (collagen I and periostin) in cocultures of EPDCs and cardiomyocytes. Immunohistochemistry indicated more membrane-bound expression of Cx43, N-cadherin, the mechanotransduction molecule focal adhesion kinase, and higher expression of the sarcoplasmic reticulum Ca^{2+} ATPase (SERCA2a). Newly developed software for analysis of directionality in immunofluorescent stainings showed a quantitatively determined enhanced cellular alignment of cardiomyocytes. This was functionally related to increased contraction. The *in vitro* effects of EPDCs on cardiomyocytes were confirmed in three reciprocal *in vivo* models for EPDC-depletion (chicken and mice) in which downregulation of myocardial N-cadherin, Cx43, and FAK were observed.

In conclusion, direct interaction of EPDCs with cardiomyocytes induced proliferation, correct mechanical and electrical coupling of cardiomyocytes, ECM-deposition and concurrent establishment of cellular array. These findings implicate that EPDCs are ideal candidates as adjuvant cells for cardiomyocyte integration during cardiac (stem) cell therapy.

INTRODUCTION

In vertebrates, cardiac development is an early embryonic event, starting with the formation of the primitive tubular heart, consisting of an endocardial layer and a myocardial layer with cardiac jelly in between. With increase in heart size and cardiac output, a stronger myocardial wall and increased myocardial perfusion is required. For this, the contribution of epicardium-derived cells (EPDCs) is indispensable. EPDCs originate from the proepicardial organ (PEO), a villous protrusion of the coelomic wall from which cells migrate through the pericardial cavity to the heart tube. Once attached to the primitive atrioventricular segment, the cells spread over the heart surface to form an transformation (EMT) subepicardial mesenchymal EPDCs are formed that migrate into the myocardium in a spatiotemporally controlled fashion (reviewed in[1]). At their final destinations they contribute to the media of the coronary arteries, the maturation of the atrioventricular cushions into fibrous valves, to the induction of Purkinje fibre formation and to myocardial architecture as interstitial fibroblasts [1,2]. The major importance of EPDCs in the establishment of myocardial maturation and cardiac remodelling has been shown in numerous studies in which defective epicardial development led to severe myocardial hypoplasia and looping disorders (e.g.[3-9]). EPDCs also provide for the cellular substrate and the extracellular matrix (ECM) component periostin needed for the development of the fibrous heart skeleton and electrical insulation between atria and ventricles [2,10].

Analysis of the cellular and molecular characteristics of EPDCs revealed their capacity to induce proliferation of fetal cardiomyocytes (CMs) by retinoic acid-dependent secretion of a trophic factor [11]. They share a common ancestor in the dorsal mesocardium with the CMs from the posterior part of the second heart field [1,9,12]. Because of the various functions they have in cardiac development, EPDCs behave as tissue-specific cardiac progenitor cells [13]. Indeed, recapitulation of part of their embryonic program, *viz*. the stabilization of coronary vessels and formation of fibrous interstitial cells could be achieved and helped to restore myocardial function when adult human EPDCs were injected into infarcted murine hearts [14]. In zebrafish, repair of myocardial injury by cardiac progenitor cells is initiated by an epicardial response [15].

These proven beneficial effects of EPDCs on myocardial injury seem to rely both on improved vascularisation, driven by thymosin β4 expression [16], and on the increase in myocardial wall thickness, in mice, and by the mobilization of cardiac progenitor cells in zebrafish. How exactly EPDCs contribute to the (re)establishment of correct myocardial architecture is largely unknown. As far as we know, this is the first study that focuses specifically on the cellular architecture of cardiomyocytes as an aspect of the interaction between EPDCs and CMs. We hypothesize that in the myocardium

EPDCs are necessary for correct arrangement and coupling of CMs, that they are required for the deposition of ECM both to give the myocardial wall the rigidity it needs, and to supply for a mechanotransduction substrate.

MATERIALS AND METHODS

Basic methodology of this study was as follows; for details see Appendix, Materials and Methods Supplement.

Cell isolation and culture

CMs were isolated from neonatal mice hearts. Cardiac fibroblasts were removed from the cultures by adherence to plastic. Non-attached cells were considered to be the CM-enriched cell population and will further be referred to as the CMs. Cells were plated at a concentration of $5x10^4$ cells per cm^2. After overnight culture, approximately 1000 quail EPDCs were added to $10x10^4$ CMs in direct coculture or in transwell cultures. EPDCs were obtained from overnight quail PEO explant cultures. EPDCs were added either as the completely explanted PEO, or as dispersed cells after overnight culture. Control cultures received an equal volume of fresh or EPDC-conditioned medium, or an equal amount of non-cardiac quail embryonic fibroblasts. Cells were cultured for one week before fixation or harvesting whole lysates for protein analysis.

CM proliferation assay

Cultures were incubated with bromo-deoxy-uridine (BrdU) the day prior to fixation and double stained for the CM marker Troponin T/C (TnT/C) and BrdU. The percentage of proliferating CMs in each culture was scored as the percentage of BrdU-positive and TnT/C-positive cells from the total number of TnT/C-positive cells. A non-paired, two-tailed Student's t-test was used for statistical comparison. A p-value of 0.05 was considered statistically significant.

Evaluation of the cultures

To study cellular differentiation and cell-cell contacts, expression of markers for CM maturation was evaluated in EPDC-CM cocultures and CM control cultures by Western blot analysis and immunohistochemistry. EPDCs were detected by staining with the quail-specific nuclear marker QCPN. Connexin 43 (Cx43) was used as a marker for electrical coupling via gap junctions, N-cadherin for mechanical coupling via adherens junctions, Troponin I (TnI) and α-actinin for sarcomeres, focal adhesion kinase (FAK) and phosphorylated FAK (FAK-P) for mechanotransduction, cardiac Ca^{2+} ATPase (SERCA2a)

of the sarcoplasmic reticulum for Ca^{2+} handling and collagen I and periostin for the ECM deposition. ECM deposition in control and CM-EPDC cocultures was further analysed by transmission electron microscopy (TEM). Contractility was evaluated in videorecordings of CM control- and CM-EPDC cultures, by measuring the displacement of the visible cellular borders at 5 positions (in the middle of each quadrant and at the center) in a frame superimposed onto the videorecordings of control CM (n=5) and experimental CM-EPDC (n=4) cultures. Displacement was expressed in the arbitrary units given by the pixel ruler. A non-paired, two-tailed Student's t-test was used for statistical comparison of 25 observations in CM-EPDC cultures and 20 observations in CM control cultures. A p-value of 0.05 was considered statistically significant.

Quantification of cellular alignment in cell cultures

Cell cultures were stained immunofluorescently for either sarcomeric TnI or Cx43 (both n=3 per experimental condition). The directionality of the staining signal in the cultures was assessed by newly developed software ("Stacks", J. Vrolijk *et al.*, unpublished software; see Appendix). Basically, 10 random digital images were recorded from each culture. The images were submitted to the Hough transformation for straight lines. The average direction could then be calculated in Hough space, as a measure of the predominant direction present in an image, while the standard deviation (SD) of the average direction could then serve as an alignment index of the cells: the lower the SD, the more the sarcomeres (in case of TnI staining) or cell membranes (in case of Cx43 staining) were aligned in the same orientation. A non-paired, two-tailed Student's t-test was used for statistical comparison. A p-value of 0.05 was considered statistically significant.

Western blot analysis

Cells from CM controls and CM-EPDC cocultures were lysed and whole cell lysates were subjected to polyacrylamide gel electrophoresis blotted onto nitrocellulose and incubated with primary and appropriate secondary antibodies. NBT/BCIP substrate conversion was analyzed densitometrically and normalized against GAPDH signal. Protein expression levels in EPDC-CM cocultures were expressed relative to the 100% control culture value.

Analysis of Cx43, N-cadherin and FAK expression after EPDC-depletion *in vivo*

The expression of gap and adherens junction proteins (Cx43 and N-cadherin), and a marker for mechanotransduction (FAK) was examined immunohistochemically after *in vivo* depletion of EPDCs, three animal models with defective epicardial development were used: the genetic antisense-Ets chicken model, [5], the mechanical proepicardial outgrowth inhibition quail model [7] and the genetic mouse podoplanin knockout model [9].

RESULTS

Quail EPDCs induce proliferation in primary cultures of neonatal CMs in a contact-dependent manner

To assess the influence of EPDCs on the proliferation of CMs, BrdU incorporation was studied in one week cultures of neonatal mouse CMs with or without a quail-derived PEO, or quail-derived EPDCs. As indicated in Figure 1, only EPDCs seeded as dispersed cells in between the CMs increased the proliferative index of the CMs modestly but significantly to 30.3 ± 9.2% compared to the proliferative index of control cardiomyocytes (18.4 ± 0.7%; see Figure 1). Complete PEO explants (i.e. naturally aggregated EPDCs) added to the CMs could not enhance CM proliferation significantly, indicating a requirement for direct cell-cell contact for induction of proliferation. This observation was confirmed by experiments in which the proliferative indexes of the CMs were not enhanced when dissociated EPDCs were added in a transwell setting (16.7 ± 4.4%) or when CMs were cultured with EPDC-conditioned medium (15.1 ± 5.1%).

Because cell numbers in the wells could affect culture characteristics, care was taken that initial seeding densities in control and cocultures (with 1% of the cells being EPDCs) were basically the same. After one week of culture, similar numbers of cells were counted in random microscopic views of control and cocultures. Cultures were double-stained for quail-specific QCPN and either Cx43 or TnI and the distribution of both CMs and EPDCs was determined. In control cultures (n=7), 66 ± 7% of the cultures consisted of CMs, the

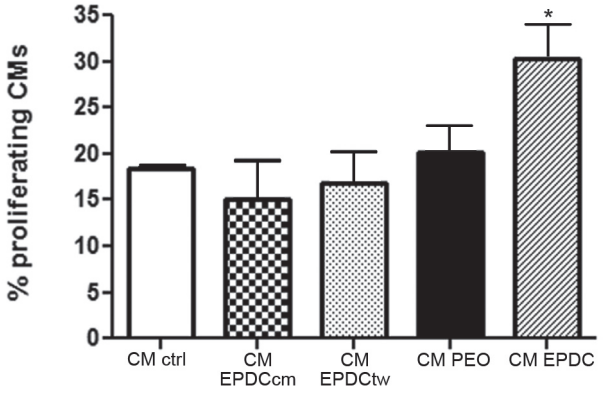

Figure 1. EPDCs induce proliferation of neonate CMs

BrdU-labelling index of TnT/C-positive CMs in cultures of control CMs (CM ctrl), and CMs cultured with either EPDC-conditoned medium (CM EPDCcm), with EPDCs in transwell culture (CM EPDCtw), with a proepicardial explant in direct contact with the CMs (CM PEO), or with dispersed EPDCs (CM EPDC). Proliferation increased significantly ($p<0.05$, *) only when CMs were in direct contact with EPDCs.

remaining 34% of the cells in culture were non-cardiomyocytes (the majority being CD31-positive endothelial (precursor) cells, and a minority of remaining fibroblasts). In the cocultures (n=7), 19 ± 7% were EPDCs, which had grown somewhat at the expense of the CMs and murine non-cardiomyocytes, making up 59 ± 6% and 22 ± 7% of the cells in coculture, respectively.
Quail-derived (i.e. EPDC-derived) double-stained QCPN- and TnI-positive cardiomyocytes were not observed in any of the cultures.

EPDCs induce directionality and enhance contraction in primary CM cultures
In CM cultures, the cells mostly showed a flattened and round appearance (Figure 2a). When cultured with a PEO explant, CMs in the direct vicinity of the explant tended to get organized in a pattern directed towards the explant (Figure 2b). Alignment of CMs in cellular arrays was observed when cocultured with EPDCs (Figure 2c,d). In the presence of EPDCs the CMs had formed parallel arrays of spindle-shaped cells, with an apparently higher TnT/C expression compared to CM control cultures. These bundles of CMs were separated by strands of TnT/C-negative, fibroblast-like proliferative cells (Figure 2d). Cellular alignment in the cultures was quantified by analyzing TnI and Cx43 immunofluorescent stainings using newly developed software (unpublished, J. Vrolijk *et al.*). In this method, the SD of the averaged sinus of the most probable lines through all pixels in the staining image served as a measure for the alignment of the cells: the lower the SD, the more the sarcomeres (in case of TnI staining) or cell membranes (in case of Cx43 staining) were aligned. Alignment increased quantitatively when EPDCs were added to the CMs, with an SD diminishing significantly from SD 38.6 ± 10.28 to SD 27.7 ± 6.7 (p=0.0002) in the case of TnI-stained cultures. When Cx43-stained cultures were analysed, increased alignment was indicated as a significantly decreased SD, from SD 35.1 ± 15.1 in CM cultures to 17.7 ± 15.4 in CM-EPDC cocultures (p=0.016).
The changes in CM morphology to more elongated cells with better alignment could not be induced by non-cardiac quail embryonic fibroblasts (QEFs). This was shown in a control experiment with “green CMs” isolated from GFP-transgenic mice, cultured with either non-cardiac QEFs or EPDCs (see Appendix). Whereas wildtype CM could be cultured as confluent layers of flat cells with a round morphology (Figure 2a), GFP-expressing CMs grew in stellate cell clusters when either no additional cells or QEFs were added (Appendix Figure 1a,c). Only when EPDCs were added in coculture, the GFP-positive CMs spreaded onto surface of the culture wells and showed a cellularly more aligned morphology after one week (Appendix Figure 1b). Synchronous contraction of functional syncytia in EPDC-CM cocultures started at day 4-5 whereas CMs alone and CMs cocultured with QEFs contracted synchronously only after 5-6 days of culture. Increased contractility in CM-EPDC cocultures was indicated by increased displacement

of visible cellular borders (2.5 ± 0.23 arbitrary pixel ruler units) compared to cell border displacement in CM control cultures (0.96 ± 0.12 arbitrary pixel ruler units; statistically significant difference, $p<0.0001$).

EPDCs induce membrane expression of Cx43, N-cadherin, and FAK as well as sarcomeric alignment in CMs

Contraction within functional cardiomyocyte syncytia was established earlier and was stronger in EPDC-CM cocultures than in CM control cultures at day 7 (see Video Appendix, contraction in CM and CM-EPDC cultures (not present in this thesis)).

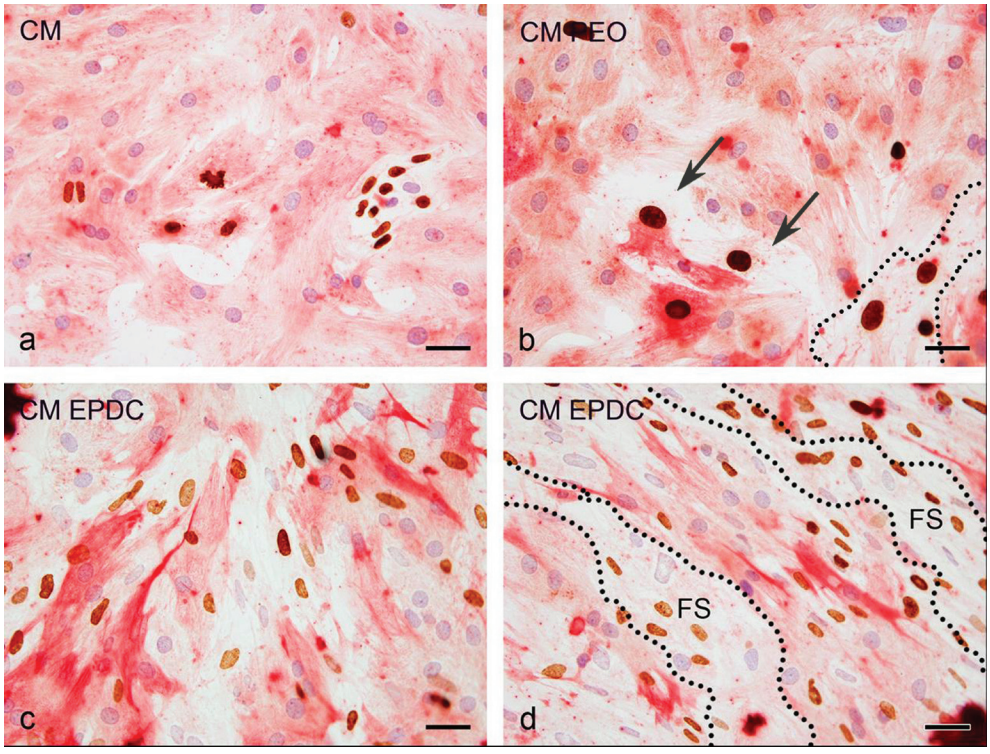

Figure 2. EPDCs affect CM morphology and orientation

Control CMs showed a flat and somewhat round appearance (a). In CM-PEO explant cultures only CMs near the explant (dotted lines and cells indicated by arrows) were elongated (b). In CM-EPDC cocultures, nearly all CMs were elongated and increased cellular array became apparent (c,d). In cocultures, fibrous cell strands isolated the cellular arrays of CMs from each other (FS; dotted lines in d). Cells were stained for BrdU (brown) and Troponin T/C (Fuchsin red) to identify proliferating CMs. Bars, 20 µm.

We investigated whether EPDC-induced enhanced contraction coincided with changes in proteins for electrical or mechanical CM coupling and contraction. As is shown in Figure 3a and 3b, both perinuclear levels of the gap junction protein Cx43 and the amount of Cx43 at the CM membranes, indicative for functional connexon formation, were increased in CMs when EPDCs were in their close vicinity. The membrane-bound increase of Cx43 was not restricted to only a few cardiomyocytes, but was observed throughout the CM-EPDC coculture as is shown in Appendix Figure 2. Also the presence of the adherens junction protein N-cadherin increased at the CM cell membrane (Figure 3e,f). TnI and α-actinin staining in EPDC-cocultured CMs reflected the enhanced alignment of

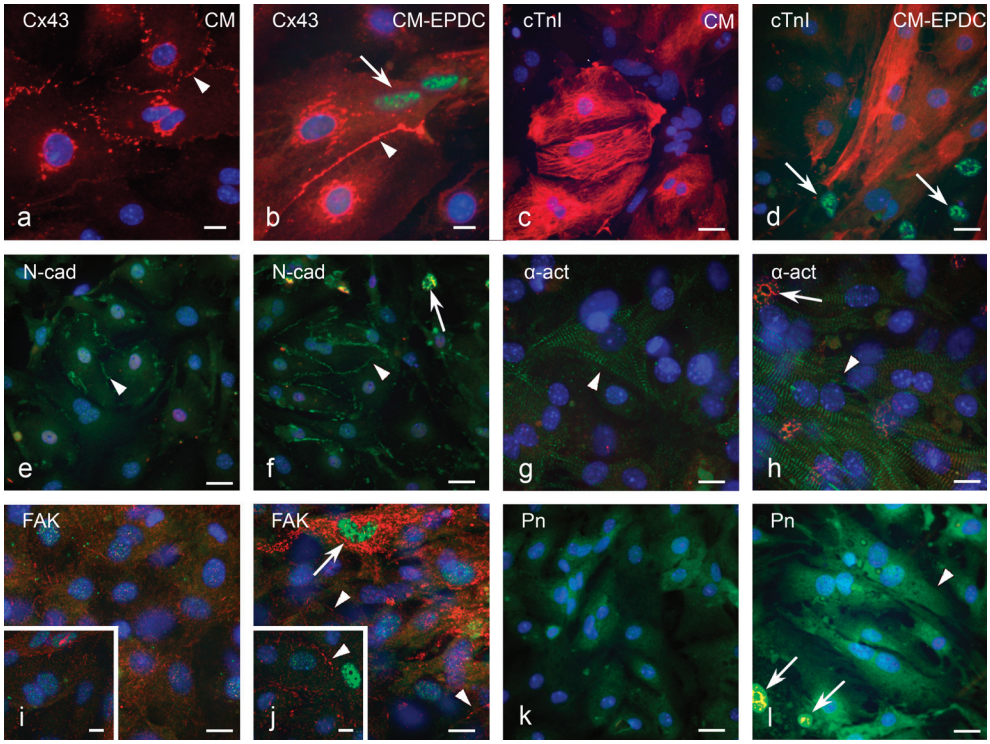

Figure 3. CM cultures (a,c,e,g,i,k) and CM-EPDC cocultures (b,d,f,h,j a,l) doublestained for quail-specific nuclear QCPN and myocardial markers

Addition of EPDCs (arrows) induced upregulation of perinuclear and membrane-bound gap junctional protein Cx43 expression (arrowheads in a,b; lower magnification overview in Appendix Figure 2), upregulation of membrane-bound adherens junctional N-cadherin (N-cad; arrowheads in e,f), and upregulation of membrane-bound FAK (arrowheads in j) and phosphorylated FAK (inserts in i,j). EPDCs were marked by high expression of FAK (arrow in j). Staining of TnI (c,d) and α-actinin (α-act; g,h) showed that contact with EPDCs changed the orientation of the sarcomeric filaments in association with the establishment of cellular array (d,h). In EPDC-CM cultures increased extracellular matrix deposition of periostin was observed (Pn; k,l). Bars, 10 μm (a,b,i,j); 20 μm (c-h;k,l).

sarcomeres in the direction of a more organized cellular array (Figure 3c,d and g,h). Upregulation of these four structural proteins in the EPDC-CM cocultures was confirmed and quantified by Western blot analysis (Figure 4). Expression levels were significantly upregulated to 120% ± 8% (Cx43), 133% ± 9% (N-cadherin), 140% ± 8.6% (TnI) and 233% ± 29.1% (α-actinin) of control levels in CM cultures.

Because coupling of CMs to surrounding cells and ECM regulates the levels of mechanotransduction by activated integrins at focal adhesions, we further analysed the effect of EPDCs in CM cultures on the key signalling molecule for integrin activation, focal adhesion kinase (FAK). EPDCs in coculture with CMs expressed FAK in a puncate pattern at their cell membranes (Figure 3i) and induced membrane-associated FAK and phosphorylated FAK (FAK-P) in the cells in their vicinity (Figure 3i,j). No increase in FAK and FAK-P expression levels was detected by Western blot analysis of culture extracts (Figure 4; expression relative to controls 91% ± 3% and 100% ± 9.4%, respectively), indicating induction of intracellular translocation of FAK and FAK-P to the cell membrane rather than increased cellular protein content.

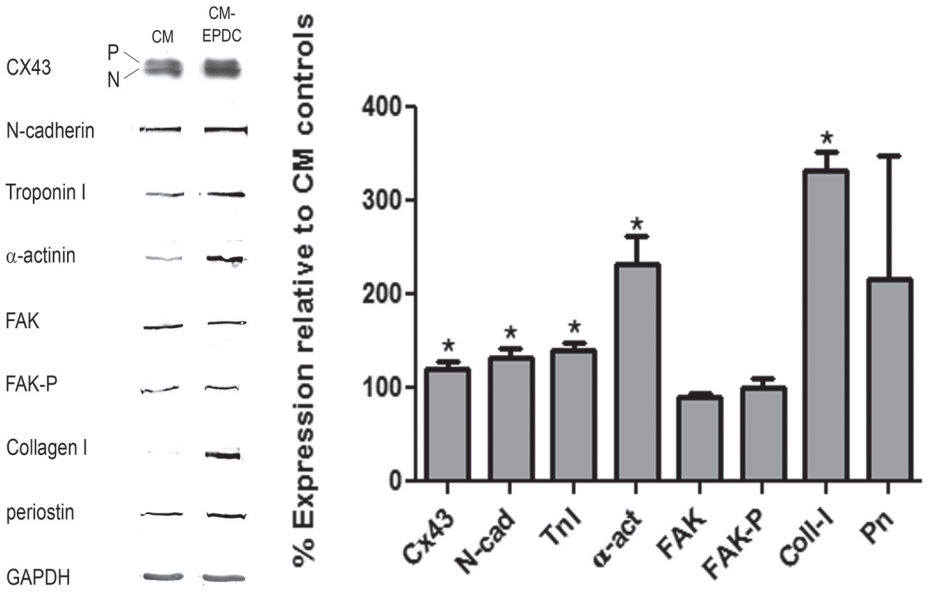

Figure 4. Western blot analysis of markers for myocardial architecture

Representative example of triplicate experiment (left panel) in which proteins for electrical coupling (Cx43), mechanical coupling (N-cadherin), sarcomeres (TnI and α-actinin), mechanosignalling (FAK and FAK-P) and ECM deposition (collagen I and periostin) were immunoblotted in cell lysates of control CM (left) and CM-EPDC (right) cocultures. Relative expression levels in CM-EPDC cocultures were normalized against GAPDH and expressed as percentage of control values with standard deviations (right panel). An asterisk indicates a value that is significantly different from the 100% control values.

In an experiment to investigate possible differences in Ca^{2+} handling, SERCA2a expression patterns were compared between controls and CMs cultured with EPDCs. Cocultured CMs showed slightly higher cellular SERCA2a expression, especially in cell-dense areas. Furthermore, the SERCA2a staining pattern seemed to be better associated with the sarcomeres (Appendix Figure 3).

EPDCs provide for ECM components in cocultures with CMs

Enhanced ECM deposition of collagen I and periostin in CM-EPDC cocultures was demonstrated by Western blot analysis (Figure 4; 333% ± 19.9% and 206% ± 133%, respectively). The ECM molecule periostin, produced by EPDCs [2], mostly colocalised with non-EPDCs (mostly CMs) in the cocultures in a diffuse pattern as if it was deposited onto the cardiomyocytes (Figure 3k,l). In order to analyse the deposition of ECM components in more detail, CM cultures and CM-EPDC cocultures were compared by transmission electron microscopy. Control CM cultures were devoid of secreted and deposited ECM (Figure 5a). Control CM cultures showed mostly young CMs characterized by high numbers

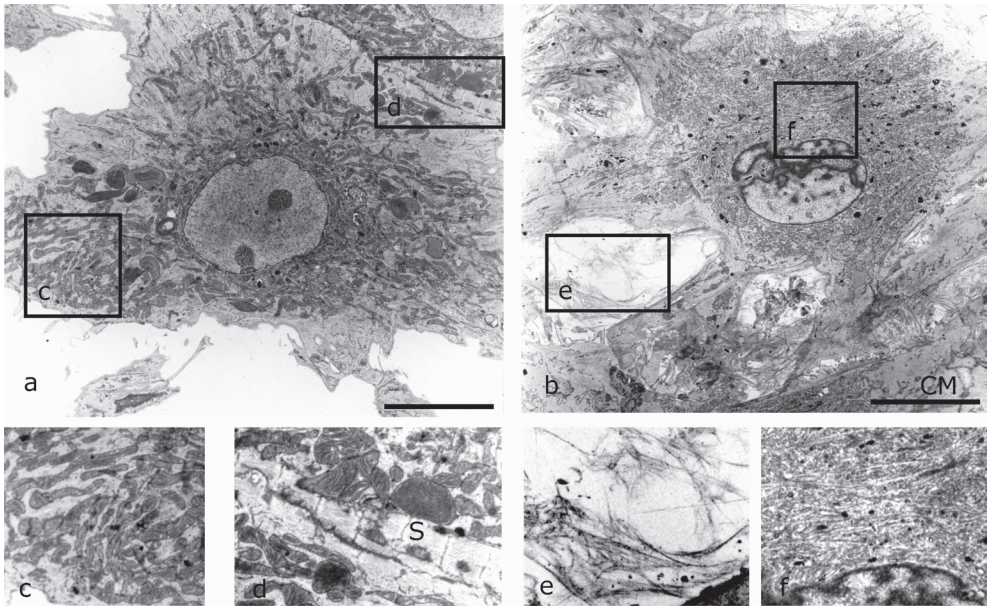

Figure 5. Transmission electron microscopy shows EPDCs as efficient ECM producers

Production and deposition of fibrous ECM components in control cultures of CMs were below detection limit in transmission electronic microscopic views (a). CM were immature showing numerous mitochondria (c) as well as developing sarcomeres (S in d). In cocultures, EPDCs (b) were in close physical contact with CMs (CM in a) and deposited fibrous ECM components into the extracellular space (e). EPDCs were characterized by the presence of abundant ER(f). Bars, 10 µm (a,b).

of mitochondria (Figure 5a,c) and immature sarcomeres (Figure 5a,d). In CM-EPDC cocultures, EPDCs were observed in close contact with CMs (Figure 5b). The EPDCs secreted and deposited high amounts of fibrous ECM components (Figure 5e) and had a highly developed rough endoplasmic reticulum (Figure 5f).

***In vivo* EPDC-depletion is associated with downregulation of Cx43, N-cadherin, FAK**

To verify whether the *in vitro* induction by EPDCs of proteins involved in architectural features as electrical coupling (Cx43), mechanical coupling (N-cadherin) and ECM-related mechanosignalling (FAK) would also occur during *in vivo* development, we used three established animal models in which the contribution of EPDCs to the myocardium was disturbed. In the podoplanin knockout mouse, upregulated E-cadherin is associated with a diminished capacity for epicardial EMT [9], in antisense Ets-1/2 treated chicken embryos EMT of the epicardium is hampered [5] and in chicken embryos with mechanically inhibited proepicardial outgrowth, epicardial outgrowth over the myocardium is prevented by a piece of eggshell membrane [7].

Because the avian expression pattern of Cx43 differs from that in mouse myocardium, we investigated only the podoplanin knockout model for the *in vivo* effect of EPDC-depletion on Cx43 expression. In normal controls, Cx43 was present predominantly in the trabecular myocardium and in the ventricular septum (Figure 6a,c,e,g). In EPDC-depleted mouse hearts, decreased Cx43 expression was observed in the left lateral wall, and especially in the ventricular septum (Figure 6a-d). Only a slight Cx43 downregulation was observed in the right ventricular wall (Figure 6f,g).

In stage HH28 chicken embryos, lower levels of N-cadherin were observed in the EPDC-depleted embryos than in the normal controls (Figure 7a-d). At stage HH35, low levels of N-cadherin were observed in control embryos (Figure 7e, g) whereas in antisense-Ets EPDC-depleted embryos, N-cadherin expression was reduced almost to background levels (Figure 7f,h). In the mouse model, N-cadherin was expressed in controls throughout the myocardium, with highest levels in the CMs just beneath the (sub)epicardium (Figure 7i,k). In the podoplanin knockouts N-cadherin staining was nearly absent (Figure 7j,l).

FAK expression was observed in control chicken embryos at stage HH28 throughout the myocardium, with highest levels in the outflow tract (Figure 8a,c). In the ventricular myocardium, FAK staining was abundant in the CMs directly adjacent to the subepicardial mesenchyme (Figure 8a,e) and in the developing trabeculae (Figure 8a,g). Epicardially inhibited embryos showed a severe reduction of FAK expression in the outflow tract (Figure 8b,d) and in the compact zone of the ventricular myocardium (Figure 8b,f), but not in the trabeculae (Figure 8b,h).

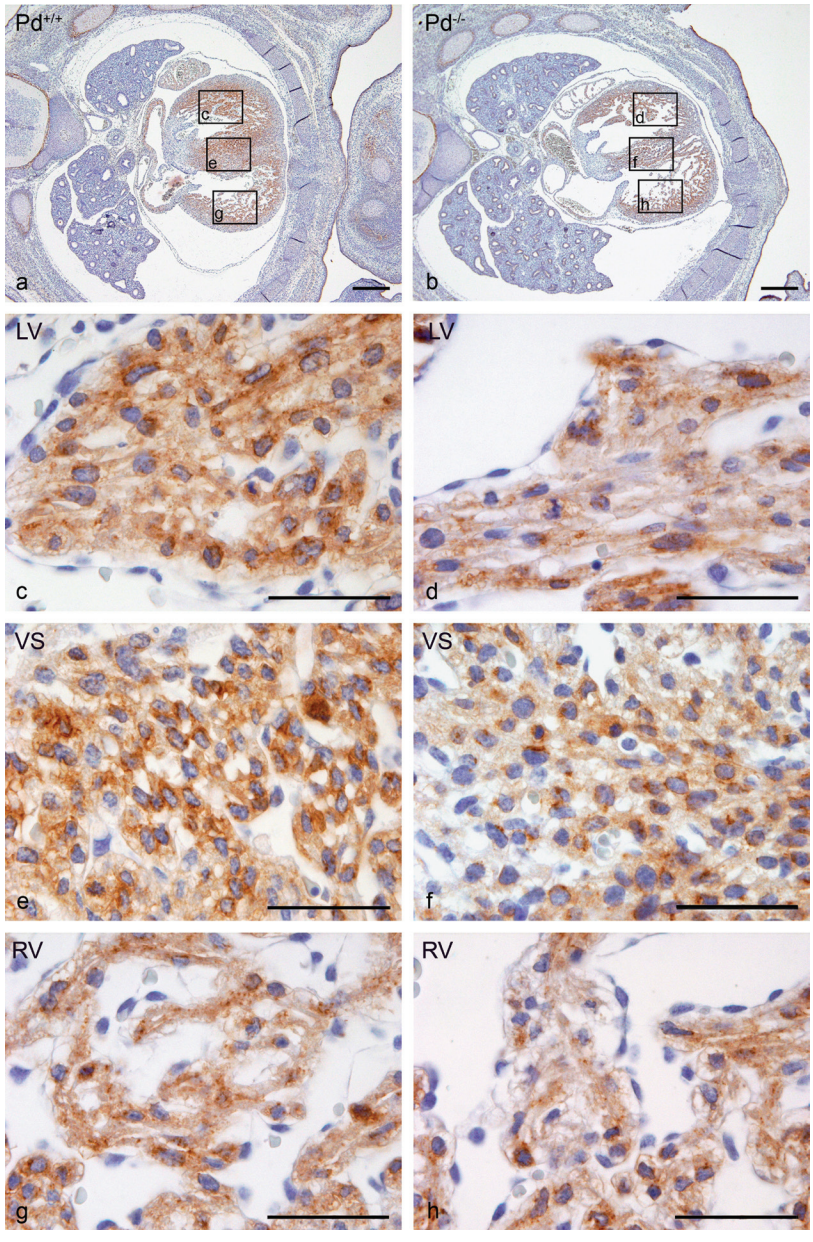

Figure 6. Cx43 staining in the podoplanin knockout mouse model for EPDC-depletion
Cx43-stained tissue sections of control (a,c,e,g) and podoplanin (Pd) knockout (b,d,f,h) mouse hearts (ED15.5). Antibody staining was visualized by a brown DAB precipitate, and cell nuclei were counterstained with blue haematoxilin. Magnifications of the boxed areas in panels a,b are indicated. Cx43 signal was decreased in the trabeculae (d,h), and the ventricular septum of the epicardially affected $Pd^{-/-}$ hearts (f) compared to control levels (c,e,g). LV, left ventricle; RV, right ventricle; VS, ventricular septum. Bars, 670 µm in a, b; 30 µm in c-h.

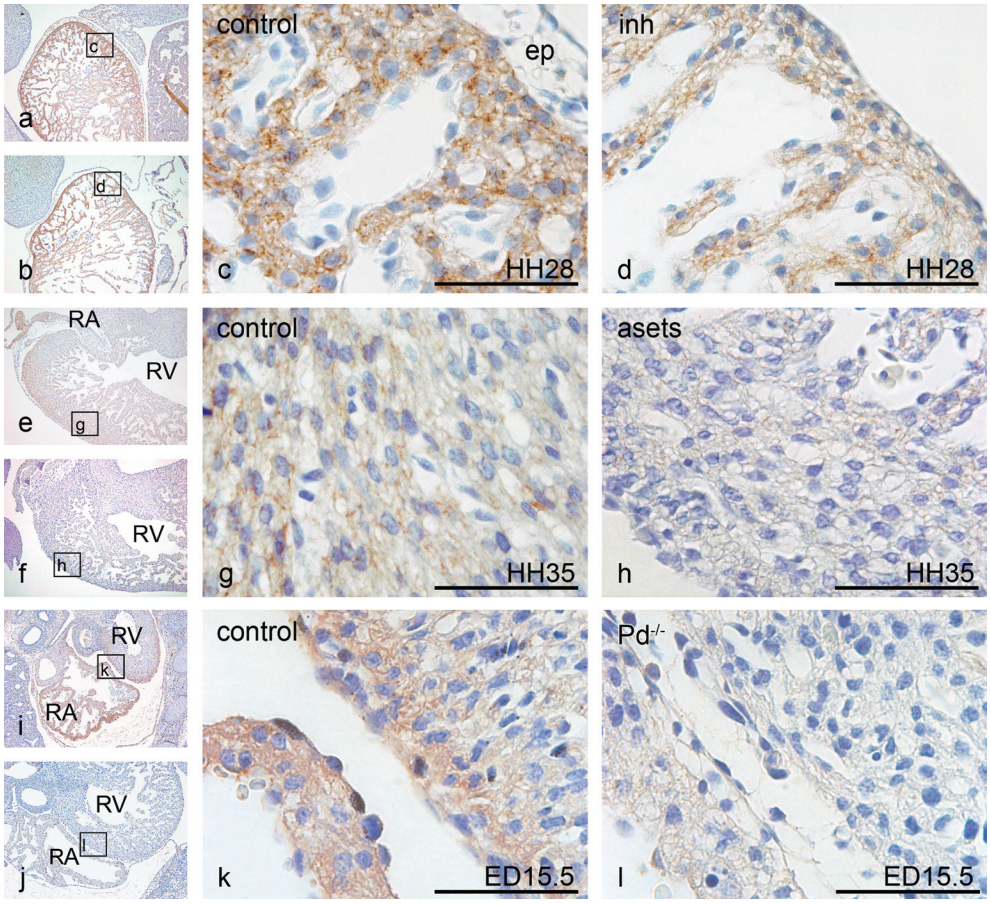

Figure 7. N-cadherin staining in three *in vivo* models for EPDC-depletion

N-cadherin stained tissue sections of three animal models for EPDC-depletion. Antibody staining was visualized by a brown DAB precipitate, and cell nuclei were counterstained with blue haematoxilin. In the quail inhibition (inh) model (a-d), proepicardial outgrowth is disturbed. Magnifications of the boxed areas (a,b,e,f,i,j) are shown (c,d,g,h,k,l). At stage HH28, N-cadherin levels were lower in the ventricular myocardium of the epicardially inhibited embryos (b,d) than in controls (a,c). In the antisense Ets1/2 (asets) model, epicardium failed to undergo EMT. At stage HH35, less N-cadherin was observed in the ventricular myocardium of asets-treated embryos (f,h) than in controls (e,g). In the podoplanin knockout ($Pd^{-/-}$) less EPDCs migrate into the myocardial wall. N-cadherin is nearly absent in the myocardium of the $Pd^{-/-}$ embryos (j,l), whereas expression levels are high in the control myocardium (i,k; arrowheads). RA, right atrium; RV, right ventricle. Bars, 200 µm in a,b; 670 µm in e,f,i,j; 30 µm in c,d,g,h,k,l.

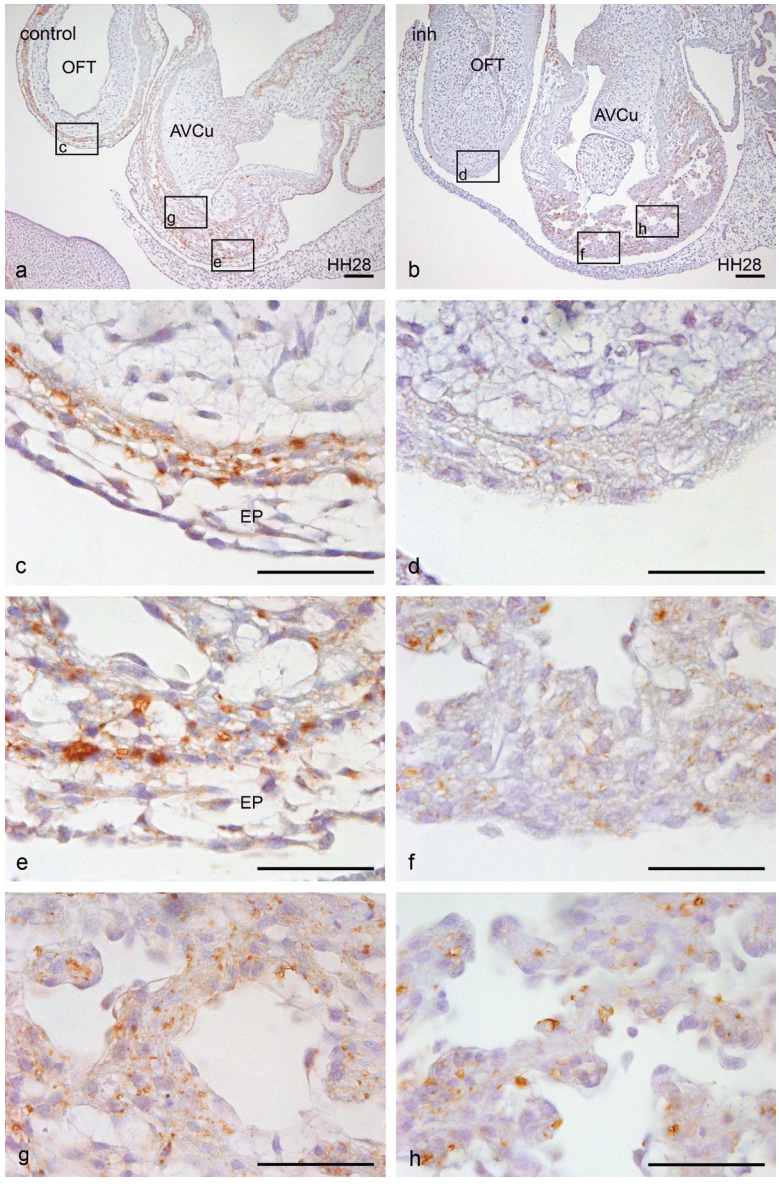

Figure 8. FAK staining after EPDC-depletion
FAK expression in the hearts of control (a,c,e,g) and epicardially inhibited (inh; b,d,f,h) chicken embryos at stage HH28. Antibody staining was visualized by a brown DAB precipitate, and cell nuclei were counterstained with blue haematoxilin. Panels c,e,g and d,f,h, are magnifications of the boxed areas in panels a and b. In the epicardially inhibited embryos, FAK expression was nearly absent in the outflow tract (*Cf.* c and d) and reduced in the compact zone of the ventricular myocardium (*Cf.* e and g). In the trabecular zone of the ventricular myocardium, FAK expression levels were hardly affected (*Cf.* g and h). AVCu, atrioventricular cushion; EP, epicardium; OFT, outflow tract. Bars, 100 µm (a,b); 30 µm (c-h).

DISCUSSION

Establishment of a mature myocardial architecture is essential for adequate myocardial function. This can be deduced from the many cardiomyopathies in which myocardial array is disturbed in association with mutations in genes encoding proteins involved in electrical and mechanical coupling, formation of and cellular attachment to the ECM, and those linked to the cytoskeleton and the cellular contractile apparatus [17]. Whereas genetic array screening is essential to increase knowledge on the protein components that cannot be missed for correct myocardial functioning, research on cellular behaviour within a developmental setting is essential to unravel how myocardial architecture is normally established and to recognize which cellular building blocks would be needed for sustained heart repair in pathological conditions. It has recently been suggested that EPDCs in particular might be related to the susceptibility for cardiomyopathies [18].

This study is one of the first to delineate the contribution of EPDCs to the cellular architecture of the myocardium. Whereas the contribution of EPDCs to coronary artery formation and stabilization has gained considerable attention over the last decades (reviewed in [1,19]), their role in the development of ventricular myocardium is far less understood. Several avian and mouse models showed that defects in epicardial development resulted in severe thinning of the compact myocardium independent of coronary arterialisation [1,5,9,20]. In these models, the spongeous appearance of the compact and septal myocardium indicated loss of myocardial array. By which regulatory mechanisms EPDCs influenced myocardial (cyto)architecture remained largely obscure.

The present study underlines that EPDCs can stimulate neonatal CM proliferation, a phenomenon that was described earlier for fetal CMs [21]. Whereas fetal CMs were able to respond to an as yet unidentified paracrine trophic factor [11], in our study neonatal CMs needed direct cell contact with the EPDCs seeded throughout the CM cultures for the induction of proliferation. Only a slight, statistically insignificant increase in proliferation was observed cocultures with PEO explants, in which only some cardiomyocytes were in direct contact with EPDCs. No increase in CM proliferation was observed in transwell cocultures and experiments with EPDC-conditioned medium. This is in line with the finding that embryonic, but not adult, cardiac fibroblasts, of which the majority derives from the epicardial lineage [1] induce CM proliferation via ECM interactions and integrin signalling[22].

Transplantation of human EPDCs to the infarcted mouse heart [14] markedly upregulated angiogenesis and improved heart function, despite the allogeneic origin of the EPDCs. In the present study, *in vitro* data concerning the influence of EPDCs on Cx43, N-cadherin and FAK expression were confirmed by reciprocal *in vivo* results in mouse and chicken models, underlining the biological relevance of our observations in the heterologous quail-mouse cocultures.

Enhanced synchronous contraction of CM strands was observed when cocultured with EPDCs. This has been documented earlier for adult rat ventricular CMs cultured with adult rat epicardial cells [23], and for neonatal CMs with cardiac fibroblasts [24]. As noted, most of these cardiac fibroblasts are in fact EPDCs [1].

In the present study, slightly earlier establishment of synchronous contraction could be due to earlier maturation of the cardiomyocytes into a functional syncytium. Although we did not determine electrophysiologically whether this was accompanied by increased conduction, we found a stronger contraction in CMs cocultured with EPDCs. This was accompanied by increased cellular and sarcomeric directionality in the cultures and could be linked to an increase in the membrane-associated expression of Cx43. Because stretch-induced mechanotransduction can also elevate membrane Cx43 levels via integrin signalling [25] it remains to be elucidated whether the increase in membrane-bound Cx43 in EPDC-CM cocultures is a cause for or a consequence of the enhanced synchronous contraction, in a coculture experiment in which both mechanical stress and functional inhibition of Cx43 connexons can be varied.

The podoplanin knockout mouse [9] served as an *in vivo* EPDC-depletion model. In these mice, penetrance for EPDC-depletion is not complete and the extent of myocardial thinning may vary. However, even in embryos with almost normal compact ventricular myocardium, a decrease in Cx43 confirmed our *in vitro* results that EPDCs are involved in the upregulation of Cx43 during CM maturation. We could not use our chicken EPDC-depletion models for this, because avian Cx43 is expressed only periarterially and subendocardially, but not in the working myocardium [26].

In addition to enhanced gap junctional coupling, we found an increase in the mechanical coupling of CMs when cocultured with EPDCs. There was more membrane-bound N-cadherin, an adherens junction protein normally present at the intercalated disks of mature CMs [27]. The immature phenotype of the early neonatal CMs was underlined by the presence of N-cadherin at all cellular borders [27]. In the reciprocal *in vivo* experiment, we confirmed the importance of EPDCs for the induction of N-cadherin expression by downregulation of myocardial N-cadherin in three animal models for EPDC-depletion (the antisense Ets-model for defective epicardial EMT [5], the mechanical proepicardial outgrowth inhibition model in chicken [7], and the EPDC-defective podoplanin knockout mouse [9]).

Because EPDCs are important for the deposition of ECM components as collagen I and periostin between and onto the CMs [1,2] we investigated whether the presence of EPDCs also increased the levels of molecules involved in mechanotransduction from the ECM, via integrin focal adhesions to signal transduction routes inside the cell. FAK was chosen as read-out molecule because it is a key component of the activated integrin complex [28]. Both in the cocultures and in the *in vivo* models we found a relation between the presence of FAK and the presence of EPDCs. Addition of EPDCs gave rise to increased membrane-

associated FAK levels, and after *in vivo* EPDC-depletion in chicken embryos myocardial FAK levels were reduced in the developing ventricular compact zone and in the outflow tract myocardium. These are sites that are normally in contact with subepicardial or interstitial EPDCs. FAK expression in the trabecular zone remained fairly intact at chicken stage HH28. This is in line with the finding that especially the compact ventricular zone is affected in our EPDC-depletion models and supports our hypothesis that the human condition of ventricular non-compaction cardiomyopathy, in which the compact zone is underdeveloped, is an epicardial problem [1]. Interestingly, deletion mutants of CM-specific integrin β1 and FAK showed a phenotype with ventricular myocardial thinning similar to that observed in several of our epicardially disturbed animal models [5,7,20,22,29]. In FAK knockouts, MEF2a, the predominant postnatal MEF2 gene product with a role in maintenance of mitochondrial content and cyto-architectural integrity [30], was identified as an important downstream target of FAK signalling.

That EPDCs affect mechanotransduction is of particular interest because recent findings showed the importance of ECM anchorage and integrin signalling by focal adhesions for the moulding of CM shape, sarcomeric alignment and electrophysiological properties [31]. Other researchers in the field of tissue engineering also emphasized how scaffold micropatterning and stiffness affect conduction velocity, sarcomeric alignment, and CM contraction force [32,33]. This is in line with our current finding that physical contact with EPDCs or at least their ECM product is necessary for proliferation of CM and further maturation of their cytoarchitecture. In fact, the effects of EPDC addition or depletion described here can largely be explained as an addition or depletion of sufficient mechanosignalling from the ECM to the CM, and may not depend on paracrine factors. Myocardial thinning and disorganization in the *in vivo* EPDC-depletion models used in this study have been described in more detail before [5,7,9]. The link with hampered mechanosignalling is that EPDC-depletion affects periostin deposition [2], with possibly consequent effects on the biomechanical properties of the ECM [34] and CM maturation in cellular arrays.

Apart from better electrical and mechanical coupling, higher contractile function in cardiomyocytes may relate to improved Ca^{2+} homeostasis and be associated with accelerated Ca^{2+} sequestration in the SR and consequent relaxation [35]. Our preliminary finding that expression of cardiac sarcoplasmic reticulum (SR) Ca^{2+} ATPase (SERCA2a) is elevated and better associated with sarcomeric patterning indicates improved Ca^{2+} handling when cardiomyocytes were cultured with EPDCs. SERCA2a is one of the key enzymes in cardiomyocyte Ca^{2+} handling; it actively transports Ca^{2+} into the SR and regulates cytosolic Ca^{2+} concentration, SR Ca^{2+} load, and the rate of contraction and relaxation of the cardiac muscle [36]. Stronger Ca^{2+} handling by the SR is a characteristic of more mature cardiomyocytes [37].

We found that non-cardiac embryonic fibroblasts do not perform like EPDCs. Thus, our data suggest that the cardiac EPDC is a specialized fibroblast, with different capacities for cellular interactions regulating CM maturation than other embryonic fibroblasts. The exact molecular mechanism through which EPDCs govern the induction of CM maturation remains to be dissected. One clue may come from the finding that the transcription factor Prox-1 leads to sarcomeric maturation in the mouse myocardium from embryonic day 12.5 onward, but not before that age [38]. This is consistent with the developmental time window at which EPDCs enter the myocardium in the embryonic mouse heart, from day 11.5 onward (A.C. Gittenberger-de Groot, unpublished observations), in quail between embryonic day 3 and 4 [39] and in human embryos between developmental week 7 and 8 (N. van Loon and H. Lie-Venema, unpublished observations). We hypothesize that the entrance of EPDCs into the underlying myocardium turns on the signalling cascades necessary for cardiomyocyte maturation either directly, by cell-cell contacts or indirectly, by the deposition of extracellular matrix components needed for signalling to the cardiomyocyte membrane and from there into the cell and its nucleus.

In conclusion, EPDCs provide the architectural clues needed for CM proliferation and maturation into an arrayed, electrically and mechanically coupled myocardium. As was shown in earlier work, they also provide paracrine factors for enhanced vascular recruitment [14,16]. Although they do not differentiate into CMs [12], EPDCs seem to be ideal and essential adjuvant cells for cardiac stem cell therapies because they provide the prerequisites for correct integration of cardiomyocytes into functional and mature cardiac syncytia.

ACKNOWLEDGEMENT

Jan Lens is kindly acknowledged for preparing the figures.

REFERENCE LIST

1 Lie-Venema H, van den Akker NMS, Bax NAM, Winter EM, Maas S, Kekarainen T, Hoeben RC, DeRuiter MC, Poelmann RE, Gittenberger-de Groot AC. Origin, fate, and function of epicardium-derived cells (EPDCs) in normal and abnormal cardiac development. ScientificWorldJournal 2007;7:1777-98.

2 Lie-Venema H, Eralp I, Markwald RR, Van Den Akker NM, Wijffels M, Kolditz DP, Van der Laarse A, Schalij MJ, Poelmann RE, Bogers A, Gittenberger-de Groot AC. Periostin expression by epicardium-derived cells (EPDCs) is involved in the development of the atrioventricular valves and fibrous heart skeleton. Differentiation 2008;76:809-19.

3 Yang JT, Rayburn H, Hynes RO. Cell adhesion events mediated by alpha 4 integrins are essential in placental and cardiac development. Development 1995;121(2):549-60.

4 Tevosian SG, Deconinck AE, Tanaka M, Schinke M, Litovsky SH, Izumo S, Fujiwara Y, Orkin SH. FOG-2, a cofactor for GATA transcription factors, is essential for heart morphogenesis and development of coronary vessels from epicardium. Cell 2000;101:729-39.

5 Lie-Venema H, Gittenberger-de Groot AC, van Empel LJP, Boot MJ, Kerkdijk H, de Kant E, DeRuiter MC. Ets-1 and Ets-2 transcription factors are essential for normal coronary and myocardial development in chicken embryos. Circ Res 2003;92:749-56.

6 Watt AJ, Battle MA, Li J, Duncan SA. GATA4 is essential for formation of the proepicardium and regulates cardiogenesis. Proc Natl Acad Sci U S A 2004;101(34):12573-8.

7 Eralp I, Lie-Venema H, DeRuiter MC, Van Den Akker NM, Bogers AJ, Mentink MM, Poelmann RE, Gittenberger-de Groot AC. Coronary artery and orifice development is associated with proper timing of epicardial outgrowth and correlated Fas ligand associated apoptosis patterns. Circ Res 2005;96:526-34.

8 Merki E, Zamora M, Raya A, Kawakami Y, Wang J, Zhang X, Burch J, Kubalak SW, Kaliman P, Belmonte JC, Chien KR, Ruiz-Lozano P. Epicardial retinoid X receptor alpha is required for myocardial growth and coronary artery formation. Proc Natl Acad Sci U S A 2005;102(51):18455-60.

9 Mahtab EA, Wijffels MC, van den Akker NM, Hahurij ND, Lie-Venema H, Wisse LJ, DeRuiter MC, Uhrin P, Zaujec J, Binder BR, Schalij M.J., Poelmann RE, Gittenberger-de Groot AC. Cardiac malformations and myocardial abnormalities in podoplanin knockout mouse embryos: correlation with abnormal epicardial development. Dev Dyn 2008;237:847-57.

10 Kolditz DP, Wijffels MC, Blom NA, van Der LA, Hahurij ND, Lie-Venema H, Markwald RR, Poelmann RE, Schalij MJ, Gittenberger-de Groot AC. Epicardium-derived cells in development of annulus fibrosis and persistence of accessory pathways. Circulation 2008;117:1508-17.

11 Kang JO, Sucov HM. Convergent proliferative response and divergent morphogenic pathways induced by epicardial and endocardial signalling in fetal heart development. Mech Dev 2005;122(1):57-65.

12 Christoffels VM, Grieskamp T, Norden J, Mommersteeg MT, Rudat C, Kispert A. Tbx18 and the fate of epicardial progenitors. Nature 2009;458(7240):E8-E9.

13 Passier R, van Laake LW, Mummery CL. Stem-cell-based therapy and lessons from the heart. Nature 2008;453(7193):322-9.

14 Winter EM, Grauss RW, Hogers B, van Tuyn J, van der Geest R, Lie-Venema H, Vicente-Steijn R, Maas S, DeRuiter MC, deVries AA, Steendijk P, Doevendans PA, van Der Laarse A, Poelmann RE, Schalij MJ, Atsma DE, Gittenberger-de Groot AC. Preservation of left ventricular function and attenuation of remodeling after transplantation of human epicardium-derived cells into the infarcted mouse heart. Circulation 2007;116(8):917-27.

15 Lepilina A, Coon AN, Kikuchi K, Holdway JE, Roberts RW, Burns CG, Poss KD. A dynamic epicardial injury response supports progenitor cell activity during zebrafish heart regeneration. Cell 2006;127(3):607-19.

16 Smart N, Risebro CA, Melville AA, Moses K, Schwartz RJ, Chien KR, Riley PR. Thymosin beta4 induces adult epicardial progenitor mobilization and neovascularization. Nature 2007;445(7124):177-82.

17 McNally E, Dellefave L. Sarcomere mutations in cardiogenesis and ventricular noncompaction. Trends Cardiovasc Med 2009;19(1):17-21.
18 Olivotto I, Cecchi F, Poggesi C, Yacoub MH. Developmental origins of hypertrophic cardiomyopathy phenotypes: a unifying hypothesis. Nat Rev Cardiol 2009;6:317-21.
19 Smart N, Dube KN, Riley PR. Coronary vessel development and insight towards neovascular therapy. Int J Exp Pathol 2009;90(3):262-83.
20 Van Den Akker NM, Winkel LC, Nisancioglu MH, Maas S, Wisse LJ, Armulik A, Poelmann RE, Lie-Venema H, Betsholtz C, Gittenberger-de Groot AC. PDGF-B signalling is important for murine cardiac development: Its role in developing atrioventricular valves, coronaries, and cardiac innervation. Dev Dyn 2008;237(2):494-503.
21 Chen TH, Chang TC, Kang JO, Choudhary B, Makita T, Tran CM, Burch JB, Eid H, Sucov HM. Epicardial induction of fetal cardiomyocyte proliferation via a retinoic acid-inducible trophic factor. Dev Biol 2002;250(1):198-207.
22 Ieda M, Tsuchihashi T, Ivey KN, Ross RS, Hong TT, Shaw RM, Srivastava D. Cardiac fibroblasts regulate myocardial proliferation through beta1 integrin signalling. Dev Cell 2009;16(2):233-44.
23 Eid H, Larson DM, Springhorn JP, Attawia MA, Nayak RC, Smith TW, Kelly RA. Role of epicardial mesothelial cells in the modification of phenotype and function of adult rat ventricular myocytes in primary coculture. Circ Res 1992;71(1):40-50.
24 van Luyn MJ, Tio RA, van S, X, Plantinga JA, de Leij LF, DeJongste MJ, van Wachem PB. Cardiac tissue engineering: characteristics of in unison contracting two- and three-dimensional neonatal rat ventricle cell (co)-cultures. Biomaterials 2002;23(24):4793-801.
25 Shanker AJ, Yamada K, Green KG, Yamada KA, Saffitz JE. Matrix-protein-specific regulation of Cx43 expression in cardiac myocytes subjected to mechanical load. Circ Res 2005;96(5):558-66.
26 Gourdie RG, Harris BS, Bond J, Justus C, Hewett KW, O'Brien TX, Thompson RP, Sedmera D. Development of the cardiac pacemaking and conduction system. Birth Defects Res 2003;69(1):46-57.
27 Hirschy A, Schatzmann F, Ehler E, Perriard JC. Establishment of cardiac cytoarchitecture in the developing mouse heart. Dev Biol 2006;289(2):430-41.
28 Mitra SK, Hanson DA, Schlaepfer DD. Focal adhesion kinase: in command and control of cell motility. Nat Rev Mol Cell Biol 2005;6(1):56-68.
29 Peng X, Wu X, Druso JE, Wei H, Park AY, Kraus MS, Alcaraz A, Chen J, Chien S, Cerione RA, Guan JL. Cardiac developmental defects and eccentric right ventricular hypertrophy in cardiomyocyte focal adhesion kinase (FAK) conditional knockout mice. Proc Natl Acad Sci U S A 2008;105(18):6638-43.
30 Naya FJ, Black BL, Wu H, Bassel-Duby R, Richardson JA, Hill JA, Olson EN. Mitochondrial deficiency and cardiac sudden death in mice lacking the MEF2A transcription factor. Nat Med 2002;8(11):1303-9.
31 Bray MA, Sheehy SP, Parker KK. Sarcomere alignment is regulated by myocyte shape. Cell Motil Cytoskeleton 2008;65(8):641-51.
32 Feinberg AW, Feigel A, Shevkoplyas SS, Sheehy S, Whitesides GM, Parker KK. Muscular thin films for building actuators and powering devices. Science 2007;317(5843):1366-70.
33 Cimetta E, Pizzato S, Bollini S, Serena E, De CP, Elvassore N. Production of arrays of cardiac and skeletal muscle myofibers by micropatterning techniques on a soft substrate. Biomed Microdevices 2009;11(2):389-400.
34 Norris RA, Damon B, Mironov V, Kasyanov V, Ramamurthi A, Moreno-Rodriguez R, Trusk T, Potts JD, Goodwin RL, Davis J, Hoffman S, Wen X, Sugi Y, Kern CB, Mjaatvedt CH, Turner DK, Oka T, Conway SJ, Molkentin JD, Forgacs G, Markwald RR. Periostin regulates collagen fibrillogenesis and the biomechanical properties of connective tissues. J Cell Biochem 2007;101:695-711.
35 Rota M, Boni A, Urbanek K, Padin-Iruegas ME, Kajstura TJ, Fiore G, Kubo H, Sonnenblick EH, Musso E, Houser SR, Leri A, Sussman MA, Anversa P. Nuclear targeting of Akt enhances ventricular function and myocyte contractility. Circ Res 2005;97(12):1332-41.

36 Periasamy M, Bhupathy P, Babu GJ. Regulation of sarcoplasmic reticulum Ca^{2+} ATPase pump expression and its relevance to cardiac muscle physiology and pathology. Cardiovasc Res 2008;77(2):265-73.
37 Korhonen T, Hanninen SL, Tavi P. Model of excitation-contraction coupling of rat neonatal ventricular myocytes. Biophys J 2009;96(3):1189-209.
38 Risebro CA, Searles RG, Melville AA, Ehler E, Jina N, Shah S, Pallas J, Hubank M, Dillard M, Harvey NL, Schwartz RJ, Chien KR, Oliver G, Riley PR. Prox1 maintains muscle structure and growth in the developing heart. Development 2009;136(3):495-505.
39 Lie-Venema H, Eralp I, Maas S, Gittenberger-de Groot AC, Poelmann RE, DeRuiter MC. Myocardial heterogeneity in permissiveness for epicardium-derived cells and endothelial precursor cells along the developing heart tube at the onset of coronary vascularization. Anat Rec 2005;282A(2):120-9.

APPENDIX

MATERIALS AND METHODS

Animals

Experiments with neonatal mice (C57bl6/OlaHsd) obtained from Harlan (Horst, The Netherlands) and ubiquitously expressing GFP transgenic mice (C57BL/6 Cr Slc TgN(act-EGFP) C14-Y01-FM131Osb; Prof. M. Okaba, Osaka , Japan) were approved by the local committee of animal experiments. Animals were maintained according to institutional guidelines; conform to those of the Federation of European Laboratory Animals Science Associations (www.felasa.eu).

Cell isolation and culture

Cardiomyocytes

Maximally 2 days old neonatal mice were decapitated and their hearts were explanted and rinsed in ice-cold sterile PBS (NPBI, Emmer Compascuum, The Netherlands). The hearts were minced and transferred into trypsin/EDTA solution (Sigma-Aldrich, St Louis, USA) and kept under continuous rotation at 4ºC for 16 h. Then the hearts were collected on a 70 µm nylon cell strainer (BD Biosciences, Bedford, USA) and transferred into a tube with 5 ml NaCl solution containing collagenase type Ia (110 U/ml) (Sigma-Aldrich, St Louis, USA) and 0.2 % BSA (Sigma-Aldrich, St Louis, USA) and incubated in a shaking waterbath at 37ºC for 3 min. The hearts were again put on a 70 µm cell strainer and the filtered cells were collected in 2 ml heat-inactivated FCS (Gibco, New York, USA) to stop collagenase activity, and 5 ml culture medium (DMEM supplemented with 10% FCS, 100 U/ml penicillin G, 100 µg/ml streptomycin and 2 mM L-glutamin; all from Gibco, Paisly, UK) was added. Then the cells were stored on ice. This step was repeated 5 times. Cells were collected and pooled by centrifugation of the tubes at 350xg for 10 min. For depletion of fibroblasts, cells were seeded at 15-20 x 10^4 living cells/cm^2 in culture flasks (Corning, Lowell, USA) and incubated at 37°C for 1 h. The non-attached cells were considered to be the cardiomyocyte-enriched cell population and will further be referred to as the cardiomyocytes.

Cardiomyocytes were cultured on glass coverslips (Menzel-Gläser, Braunschweig, Germany) in 24-wells plate (Corning) precoated with fibronectin (10 µg/ml; Harbor Bioproducts, Norwood, USA) dissolved in PBS containing 1% gelatin. Fibronectin was cross-linked using 0.5% glutaraldehyde (Merck, Darmstadt, Germany). Cells were plated at a concentration of 5x10^4 cells per cm^2 in culture medium. After 24 h the plates were washed

with warm PBS to remove non-attached and dead cells. Then cells were used for co-culturing with EPDCs or QEFs. The medium was replaced every 2 days during culture.

Proepicardial organs (PEO) explants and epicardium-derived cells (EPDCs)

Quail proepicardial organ explants were isolated from Hamburger and Hamilton (HH;[1]) stage 15-17 embryos as described previously[2] and cultured overnight in Primaria culture wells (BD Biosciences, San Jose, USA) in M199 (Earl's salt - L-glutamine - HEPES; Life Technologies, Invitrogen, Carlsbad CA, USA) supplemented with 10% FCS ITS (insulin, transferrin and selenium-G; Gibco, Invitrogen, Carlsbad CA, USA), pen/strep and gentamycin (all Invitrogen). PEO explants were either dissociated from the well with trypsin (Sigma, T3924) for 3 minutes to obtain the complete PEO for coculture with CMs, or for 10 minutes to obtain isolated (dispersed) EPDCs.

Quail embryonic fibroblasts (QEFs)

Thoraxes from which the heart was excised were obtained from stage HH30-35 quail embryos. The thoracic region without heart and lungs was minced and tissue fragments of three pooled thorax specimens were dissociated in trypsin-EDTA (Sigma, T3924) for 5-7 min, centrifuged (10 min at 1000 rpm) The pellet was resuspended and plated in 6-wells plates (Corning) in DMEM culture medium (Low 1g/L D-glucose, + L-glutamine, 25 mM Hepes and pyruvate; Life technologies - Gibco / Invitrogen; supplemented with 10% inactivated FCS and 1% pen/strep). After 24 hours, any remaining tissue fragments were removed and the QEFs were allowed to expand for another 48 - 72 hours, and dissociated with trypsin for 10 minutes.

Coculture experiments

For coculture experiments EPDCs derived from 1 PEO (estimated to consist of approximately 1000 cells) were added to the cardiomyocyte culture wells, each seeded with $5x10^4$ cardiomyocytes 24 h before adding EPDCs. The plates were washed with warm PBS to remove non-attached cardiomyocytes just before adding EPDCs. Mouse cardiomyocytes and quail EPDCs were cocultured on fibronectin-coated glass slides, and in transwell cultures with EPDCs seeded in the upper compartment of the transwell (Corning-Costar, Cambridge, MA). Cardiomyocytes were also cultured with EPDC-conditioned medium. EPDC-conditioned medium was harvested from 5-10 day old PEO cultures. Cells from PEO explants undergo EMT and consist predominantly of mesenchymal EPDCs after 5 days in culture. Green eGFP cardiomyocytes were cocultured with EPDCs as described above. For fibroblast control cultures, 1000 QEFs were added instead of the approximately 1000 dispersed EPDCs. Cell cultures were fixated with 4% PFA in PBS for 15 minutes and kept in 70% ethanol at 4ºC until use for immunohistochemistry.

Cardiomyocyte proliferation assay

Fibroblast-depleted cardiomyocytes cultured as control cultures, in coculture with quail PEO explants or EPDCs, or in transwell experiments as described above, were incubated with 1 μM bromo-deoxy-uridine (BrdU; Sigma-Aldrich) for 24 h at culture day 6. Cells were fixed with 4% paraformaldehyde for 15 minutes and stored in 70% ethanol till double staining for troponin T/C and BrdU as described below. After staining, the percentage of proliferating cardiomyocytes in each culture was scored as the number of BrdU-positive and TnT/C-positive cells divided by the total number of TnT/C-positive cells, counted in 25 microscopic fields at 100X magnification. A non-paired, two-tailed Student's *t*-test was used for statistical comparison between cardiomyocyte proliferation indexes under control and experimental culture conditions. A p-value of 0.05 was considered statistically significant.

Immunohistochemistry

For double staining of BrdU and troponinT/C, cells were pre-incubated with 0.5% Triton-X100 and 1% BSA (both Sigma-Aldrich, Saint Louis, USA) for 15 min and then stained with goat-anti-human troponin T-C (clone C-19; Santa Cruz Biotechnology, Santa Cruz, USA; diluted 1:10) at 4˚C overnight. After washing with PBS, a secondary rabbit-anti-goat antibody conjugated with alkaline phosphatase (Zymed, South San Francisco, USA; diluted 1:100) was added. Troponin binding was visualized using Fuchsin (Dakocytomation, Carpinteria, USA) as a substrate. Then, endogenous peroxidase was blocked with 0.5% phenylhydrazin for 30 min, at 37°C. After rinsing the slides with PBS, the slides were incubated with 0.7 M HCl for 25 min. BrdU antigen retrieval was performed by incubation with 0.05% pepsin (Sigma-Aldrich) in 0.35 M HCl at 37˚C for 10 min. Pepsin activity was blocked with 5% BSA and 0.5% Tween 20 (Sigma-Aldrich, Saint Louis, USA). Endogenous avidin and biotin were blocked using an avidin/biotin blocking kit according to the manufacturer's protocol (Vector Labs, Burlingame, USA), and cells were incubated with anti-BrdU monoclonal antibody (clone BU33, Sigma-Aldrich; diluted 1:100) at room temperature for 1 h. Biotinylated goat-anti-mouse IgG1 antibody (Southern Biotech, Birmingham, USA; diluted 1:100) was used as secondary antibody, followed by streptavidin-peroxidase (Dako, Glostrup, Denmark; diluted 1:100). Presence of BrdU was visualized with diaminobenzidin (DAB; Sigma-Aldrich, Saint Louis, USA). Photomicrographs of the stained culture slides were recorded using an Olympus AX70 light microscope and Olympus DP-12 digital camera.

Quail-derived EPDCs in the cultures were visualized by immunofluorescence microscopy using the monoclonal quail-specific nuclear antibody QCPN (Hybridoma bank, diluted 1:4) followed by FITC-conjugated goat-anti-mouse secondary antibody (ITK Diagnostics, Uithoorn, The Netherlands; diluted 1:50) or a rabbit-anti-mouse TRITC-conjugate (DAKO,

Glostrup, Denmark; diluted 1:200). To study cellular differentiation and cell-cell contacts antibodies directed against connexin 43 (Cx43; rabbit polyclonal C-6219, Sigma-Aldrich, Saint Louis, USA; diluted 1:200), N-cadherin (monoclonal, C-3865, Sigma-Aldrich, Saint Louis, USA; diluted 1:250), cardiac Troponin I (TnI; goat polyclonal SC-8118, Santa Cruz Biotechnology, Santa Cruz, CA, USA; diluted 1:200), alpha-actinin (Sigma clone EA53), focal adhesion kinase (FAK(A17); SC-557, Santa Cruz Biotechnology, Santa Cruz, CA, USA; diluted 1:200), and periostin ([3]; diluted 1:200) were used, followed by visualization with goat-anti-rabbit AlexaFluor568 (Molecular Probes, Leiden, the Netherlands) for Cx43 and rabbit-anti-goat AlexaFluor568 (Molecular Probes, Leiden, The Netherlands) for TnI. Binding of N-cadherin, periostin and sarcoplasmic reticulum Ca^{2+} ATPase (SERCA2a; Affinity BioReagents, Golden CO, USA; diluted 1:200) was visualized by secondary incubation with biotin-conjugated antibodies (horse-anti-mouse, BA-2000; horse-anti-goat, BA-9500 and goat-anti-rabbit, BA-1000, all Vector Labs, Burlingame, USA; diluted 1:200) followed by avidin-D-fluorescein-FITC (A-2001, Vector Labs). Digital photomicrographs of immunofluorescent staining were recorded using a Leica DM Irbe microscope (Leica Microsystems B.V., Rijswijk, The Netherlands) , connected via a BD Carve II unit (BD, Franklin Lakes NJ, USA) to a Rolera-MGI Fast1394 camera (QImaging, Surrey BC, Canada), Recordings were processed to image files using Image-Pro 6.2 sofware (MediaCybernetics, Bethesda, MD, USA). For SERCA2a photomicroscopy; Appendix Figure 3) an Olympus AX70 microscope connected to a 2Mp Slider camera (model 25.4, Diagnostics Instruments Inc., Sterling Heigts, MI , USA) was used in combination wit SPOTadvanced Imaging Software (Diagnostics Instruments Inc., Sterling Heigts, MI , USA). For each separate staining, photomicroscopy of control and experimental cell cultures was done with exactly the same exposure settings (and only for the recordings of SERCA2a staining, ImageJ background subtraction) to ensure comparability.

Quantification of cellular alignment in cell cultures

Cell cultures were stained immunofluorescently for either sarcomeric TnI or Cx 43. The directionality of the staining signal in the cultures was assessed by newly developed software (“Stacks”, J. Vrolijk, A.K. Brouwer, R.W. Dirks en H.J. Tanke; unpublished software). Basically, 10 random digital photomicrographs were recorded from each culture. The images of each photomicrograph were submitted to the Hough transformation for straight lines. Each staining-positive pixel contributes thereby a sinus to the Hough space (r, θ), which corresponds to all possible straight lines from which the pixel can be part of. The threshold to determine positive staining was set at the same level in all measurements. The parameters r and θ are the distance- and direction-axis, respectively, corresponding to the parameters of the normal form of the equation for straight lines. The Hough transform of a complete image represents the probability of straight lines, as function of

r and θ, present in the image. The average direction could then be calculated in Hough space, as a measure of the predominant direction present in a photomicrograph, while the standard deviation (SD) of the average direction can then serve as a measure for the alignment of the cells: the lower the SD, the more the sarcomeres (in case of TnI staining) or cell membranes (in case of Cx43 staining) were aligned. The SD after Hough transformation was determined both in Cx43 stained cultures and TnI-stained cultures (n=3 for each staining, both for experimental and control cultures).

Western blot analysis

Cells from cardiomyocyte controls (n=9) and cardiomyocyte-EPDC cocultures (n=9) were lysed in RIPA buffer (Pierce, 89900) with protease inhibitor cocktail (Sigma, P8340). Immunoblotting was performed in triplicate with cell extracts (n=3; each from 3 pooled cell culture lysates). Whole cell lysates (10 or 20μg/lane) were subjected to 10% sodium dodecyl sulphate-polyacrylamide gel electrophoresis (SDS-PAGE), blotted onto nitrocellulose, and incubated for 1 hr with primary antibodies. Alkaline phosphatase-conjugated secondary antibodies and NBT/BCIP substrate (Bio-Rad, VA) were used for detection. Densitometric analysis was performed using ImageJ version 1.41 (Research Services Branch, National Institute of Mental Health, Bethesda, MD). Values of each Western blot signal obtained from Image J were normalized against GAPDH and were expressed as a percentage of the control value. Primary antibodies used were anti-Cx43 (Invitrogen 71-0700; diluted 1:100), anti-N-cadherin (Abcam Ab182030; diluted 1:1000), anti-Troponin I (Abcam Ab64327; diluted 1:500), anti-α-actinin (Sigma A 2543; diluted 1: 500), anti-FAK (SC-557, Santa Cruz Biotechnology, Santa Cruz, USA; diluted 1:250), anti-FAK-P (Invitrogen, 44624G; diluted 1:250), anti-collagen I (Southern Biotech 1310-01; diluted 1:500), anti-periostin ([3]; diluted 1:200), and anti-GAPDH (Serotec AHP996, diluted 1:500) as a control for protein loading. Secondary antibodies used were goat-anti-rabbit AP (Immunoresearch Laboratories, diluted 1:1500) and donkey-anti-goat AP (Abcam Ab6886), diluted 1:1000).

Electron microscopy

Cells cultured for 7 days in culture plates were fixed with 2% glutaraldehyde cells and post-fixed in 1% osmium tetra-oxide. After dehydration in a graded series of ethanol, cells were embedded in Epon 812 (Serva, Heidelberg, Germany). Ultrathin sections were cut and stained with uranyl acetate and lead citrate and examined with a transmission electron microscope (Philips 201) at 60 kV.

Analysis of Cx43, N-cadherin and FAK expression after EPDC depletion *in vivo*

To examine the expression of adherens and gap junction proteins after *in vivo* depletion of EPDCs, three animal models were used. In the genetic antisense-Ets chicken model, retrovirally transduced antisense-Ets1/2 hampers epicardial EMT [4]. In the mechanical proepicardial outgrowth inhibition quail model, a piece of eggshell membrane obstructs outgrowth of epicardium over the heart tube [5,6]. In the genetic mouse podoplanin knockout model, epicardial EMT is disturbed[7]. Antisense Ets-1/2 embryos (HH 35, n = 3), inhibition embryos (HH28 and HH40, n= 3 for each developmental stage) and mouse podoplanin knockout embryos (ED 15.5, n=3) and their respective age-matched, untreated or wild-type controls (n=3 in each control set) were sectioned as described before [4]. Sections were stained with the antibodies described above under "Immunohistochemistry". Binding of N-cadherin (diluted 1:250) and Cx-43 (1:200) was visualized using horse-anti-mouse biotin (BA-2000, Vector Labs, Burlingame, USA; diluted 1:200) and goat-anti-rabbit biotin (BA-1000, Vector Labs, Burlingame, USA; diluted 1:200), respectively, followed by Vectastain ABC peroxidase labelling (PK-6100, Vector Labs, Burlingame, USA) according to the manufacturers protocol and DAB precipitation. Sections were examined by light microscopy and photomicrographs were recorded using a Olympus AX-70 microscope in combination with an Olympus DP12 camera. For each particular antibody staining, microscope and camera settings were identical for the recording of sections of control and experimental embryos.

RESULTS

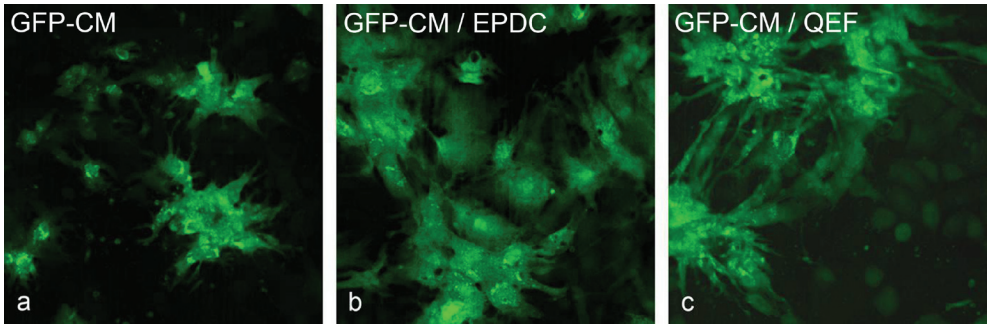

Appendix Figure 1. EPDCs are a specialized fibroblast population
CMs isolated from ubiquitously eGFP expressing "Green mice" were isolated and cultured for one week as indicated in the Appendix Materials and Methods Supplement (a). The GFP-positive CMs grew in stellate cell aggregates (n=5), phenotypically different from the flat, squamous phenotype of cultured wild-type CMs (*Cf.* Figure 2a in the main text) (a). Addition of EPDCs to the GFP-CM cultures induced spreading and alignment of the green CMs (n=3) (b). Non-cardiac quail embryonic fibroblasts (QEFs), were not able to induce cardiomyocyte spreading and alignment (n=4) (c). CMs cultured with QEFs (c) grew in similar stellate cell aggregates as the control cultures (a).

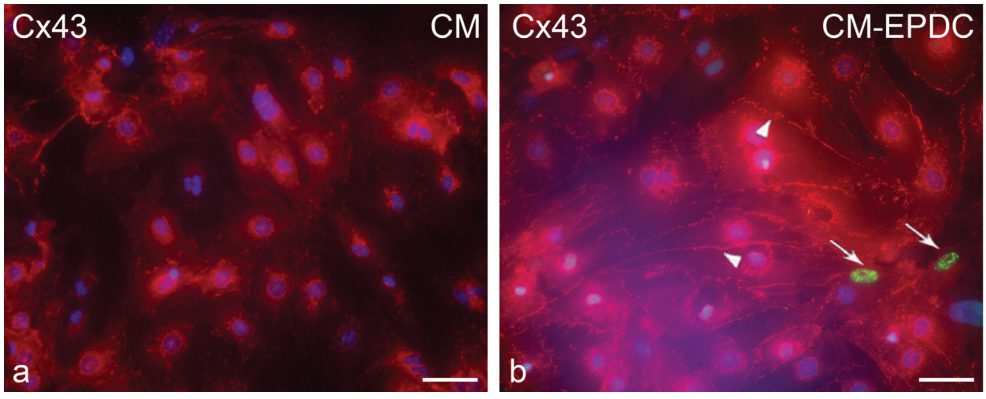

Appendix Figure 2. Cx43 membrane expression is upregulated in CM-EPDC cocultures
Overview photomicroscopy showing that both the perinuclear and the membrane-bound increase of Cx43 (red marker, arrowheads) is not restricted to only a few cardiomyocytes, but is observed throughout the CM-EPDC coculture. a) Control CM culture; b) CM-EPDC coculture with EPDCs marked by QCPN (green nuclei). Bar, 40 µm

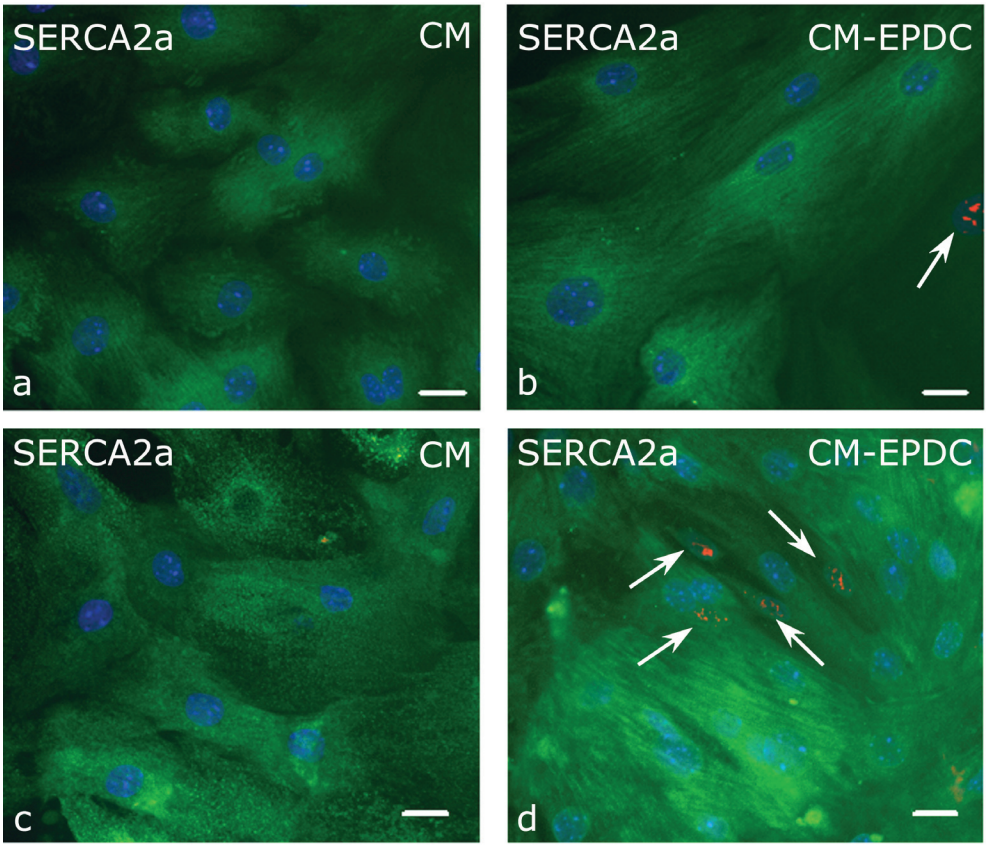

Appendix Figure 3. SERCA2a staining indicating differences in Ca^{2+} homeostasis
Compared to its levels in CM control cultures (a,c), SERCA2a expression (green signal) is slightly higher and seemingly more confined to the sarcoplasmic reticulum surrounding the sarcomeres in CM-EPDC cocultures (b,d), especially in culture areas with a higher cell density (d). EPDCs were identified by a red nuclear QCPN staining (arrows). Bar, 20 µm.

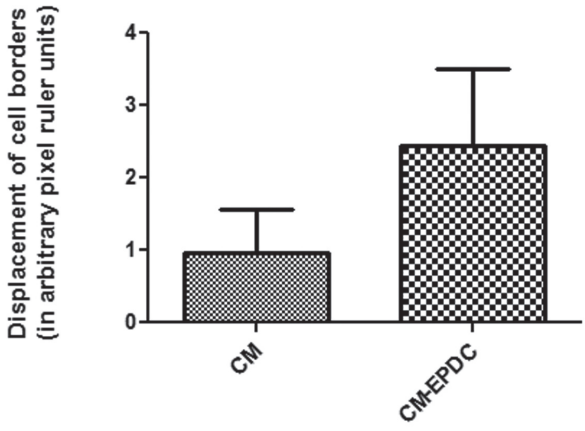

Appendix Figure 4. Quantification of increased contraction in CM-EPDC cocultures
Displacement of cell borders was taken as a measure for contractility and quantified in videorecordings (e.g. as those in Video Appendix (not present in this thesis)) of CM control cultures and CM-EPDC cocultures as described in the Materials & Methods section. A statistically significant ($p<0.0001$) increase in contractility was observed in CM-EPDC cocultures.

REFERENCE LIST

1 Hamburger V, Hamilton HL. A series of normal stages in the development of the chick embryo. J Morphol 1951;88:49-92.

2 Gittenberger-de Groot AC, Vrancken Peeters M-PFM, Mentink MMT, Gourdie RG, Poelmann RE. Epicardium-derived cells contribute a novel population to the myocardial wall and the atrioventricular cushions. Circ Res 1998;82:1043-52.

3 Kern CB, Hoffman S, Moreno R, Damon BJ, Norris RA, Krug EL, Markwald RR, Mjaatvedt CH. Immunolocalization of chick periostin protein in the developing heart. Anat Rec 2005 May;284A(1):415-23.

4 Lie-Venema H, Gittenberger-de Groot AC, van Empel LJP, Boot MJ, Kerkdijk H, de Kant E, DeRuiter MC. Ets-1 and Ets-2 transcription factors are essential for normal coronary and myocardial development in chicken embryos. Circ Res 2003;92:749-56.

5 Eralp I, Lie-Venema H, DeRuiter MC, Van Den Akker NM, Bogers AJ, Mentink MM, Poelmann RE, Gittenberger-de Groot AC. Coronary artery and orifice development is associated with proper timing of epicardial outgrowth and correlated Fas ligand associated apoptosis patterns. Circ Res 2005 February 10;96:526-34.

6 Männer J. Experimental study on the formation of the epicardium in chick embryos. Anat Embryol 1993;187:281-9.

7 Mahtab EAF, Wijffels MCEF, van den Akker NMS, Hahurij ND, Lie-Venema H, Wisse LJ, DeRuiter MC, Uhrin P, Zaujec J, Binder BR, Schalij M.J., Poelmann RE, Gittenberger-de Groot AC. Cardiac malformations and myocardial abnormalities in podoplanin knockout mouse embryos: correlation with abnormal epicardial development. Dev Dyn 2008;237:847-57.